Sensors and Actuators B 215 (2015) 39–44

Contents lists available at ScienceDirect

Sensors and Actuators B: Chemical

journal homepage: www.elsevier.com/locate/snb

High triethylamine-sensing properties of NiO/SnO_2 hollow sphere P–N heterojunction sensors

Dianxing Ju[a,b], Hongyan Xu[a,b,*], Qi Xu[a,b], Haibo Gong[a,b], Zhiwen Qiu[a,b], Jing Guo[a,b], Jun Zhang[a,b], Bingqiang Cao[a,b,*]

[a] School of Materials Science and Engineering, University of Jinan, Key Laboratory of Inorganic Functional Materials in Universities of Shandong, Jinan 250022, Shandong, China
[b] Shandong Provincial Key Lab of Preparation and Measurement of Building Materials, University of Jinan, Jinan 250022, China

ARTICLE INFO

Article history:
Received 18 December 2014
Received in revised form 1 March 2015
Accepted 9 March 2015
Available online 17 March 2015

Keywords:
SnO_2 hollow spheres
NiO
P–N heterojunction
TEA sensor

ABSTRACT

Triethylamine (TEA) gas sensor with high response and selectivity was fabricated successfully with PN heterojunction consisted of n-type SnO_2 hollow spheres and p-type NiO nanoparticles. SnO_2 hollow spheres were synthesized by a template-assisted hydrothermal method. The NiO/SnO_2 P–N junction was formed by depositing NiO nanoparticles onto the surface of SnO_2 hollow sphere sensors via a pulsed laser deposition (PLD) process. The response of NiO/SnO_2 sensor is up to 48.6 when exposed to 10 ppm TEA gas, which is much higher than that of pristine SnO_2 hollow spheres and most of other reported TEA sensors. The detection limit can also be as low as 2 ppm-level. Moreover, the optimal operating temperature is down to 220 °C, and 40 °C lower than that of the pristine SnO_2 hollow sphere sensor. These good sensing performances mainly attribute to the formation of depletion layer at the P–N junction interface in the NiO/SnO_2 sensor, which makes great variation of resistance in air and TEA gas. Thus, the combination of n-type SnO_2 hollow spheres and p-type NiO nanoparticles provides an effective strategy to design new TEA gas sensors.

1. Introduction

Triethylamine (TEA) is an explosive and excitant gas, which has been widely used as catalyst, preservatives, organic solvents and synthetic dyes in industry [1,2]. It exhibits a great damage on health, such as skin burns, headaches, and pulmonary edema when the concentration is more than its threshold of 10 ppm on volumetric basis (ppmV) in air [2]. Moreover, it also endangers our environment when its steam is mixed with air and exposed to the flame [2,3]. Although some traditional methods like gas detection tube and chromatography methods are powerful for TEA detection, the complex detection process and expensive equipment hinder their wide applications [1,4,5]. Thus, there is a strong demand of simple and portable TEA sensor with high response and good selectivity in order to monitor the real environment.

SnO_2 is generally well-known as a wide band gap n-type oxide semiconductor with a direct band gap of 3.6 eV [6,7]. It has been widely used for catalysts [8], lithium ion batteries [9] and transparent electrodes [10], especially in combustible and toxic gas detection devices (gas sensors) [11,12]. Previous reports have demonstrated that SnO_2-based gas sensors exhibit good response to many toxic gases like H_2S [13], CO [14] and volatile organic gas [15]. However, gas sensors based on SnO_2 for detection of TEA are rarely reported. To the best of our knowledge, only Wang et al. [16] fabricated SnO_2 nanorods sensor to detect TEA with a response of 200 to 1000 ppm TEA at 350 °C. Then, Liu et al. [17] prepared SnO_2 submicron rods and the response was as low as 11–450 ppm TEA gas. Clearly, their sensing response needs to be further improved.

It is well know that the sensing properties of nanomaterials are directly related to their structure and morphology. Taking above factors into account, hollow nanospheres have been proved to be a preferred structure due to their large surface area, efficient catalytic activity, and structural stability [18,14,19]. In addition, the introduction of noble metal particles or hetero-junction has also been reported to be an alternative way to improve sensing properties [20–22]. Thus, many efforts have been carried out to enhance their sensing performance. For example, Hong et al. [23] synthesized Pd-loaded SnO_2 yolk–shell nanostructures for methyl benzene. The sensors exhibited an unusually high response and selectivity to methyl benzenes, with very low cross-responses

* Corresponding authors at: School of Materials Science and Engineering, University of Jinan, Key Laboratory of Inorganic Functional Materials in Universities of Shandong, Jinan 250022, Shandong, China.
E-mail addresses: mse_xuhy@ujn.edu.cn (H. Xu), mse_caobq@ujn.edu.cn (B. Cao).

http://dx.doi.org/10.1016/j.snb.2015.03.015
0925-4005/

to various interfering gases. This made them suitable for precise monitoring of indoor air quality. Recently, our group synthesized NiO/ZnO nanosheet heterostructures and the sensing response was enhanced obviously compared with pristine ZnO sensor [22]. The enhancement of their performance could be attributed to the formation of P–N heterojunction at the interface of NiO/ZnO.

In here, a p-type NiO/n-type SnO_2 heterojunction TEA sensor was designed, where NiO nanoparticles were implanted onto the surface of SnO_2 hollow sphere sensors by a pulsed laser deposition (PLD) method. NiO is a p-type oxide semiconductor with a bandgap of 3.4 eV and easily forms P–N heterojunctions with n-SnO_2 [24,25]. After the formation of P–N junctions, the sensing performances to TEA are enhanced obviously compared with the reported data, which indicates a great potential application in detecting TEA.

2. Experimental

2.1. Synthesis of SnO_2 hollow spheres and NiO/SnO_2 heterostructure

All chemicals were purchased from Sinopharm Chemical Reagent (Shanghai, China). In a typical synthesis, 8 g of glucose was dissolved in deionized water (40 ml) under vigorous magnetic stirring. Then, the solution was transferred into a 50 ml Teflon-lined autoclave, and maintained at 180 °C for 6 h in order to obtain carbon microspheres. After centrifugation, the product was dispersed into 100 ml ethanol followed by adding 4.5 g $SnCl_2{\cdot}2H_2O$ into above mixture with assistance of ultrasonication to ensure the sufficient diffusion of Sn^{2+} onto surface of carbon spheres, due to the hydrogen bond interactions. The obtained sample was rinsed with deionized water and absolute ethanol several times. Afterwards, it was dried at 70 °C, followed by calcinations at 500 °C for 2 h. The as-prepared SnO_2 hollow spheres were dispersed into deionized water to form a paste and then coated onto the outside surface of alumina tubes. Afterward, a thin layer of p-type NiO nanoparticles was deposited onto the surface of SnO_2 hollow spheres by PLD. The typical PLD growth condition for NiO is as following. A KrF laser of 1 mJ/cm^2 and an oxygen partial pressure of 3×10^{-4} Pa were typically applied. The alumina tubes with SnO_2 hollow spheres were fixed on the substrate. By controlling the 3000 laser pulses with 5 Hz frequency, the NiO nanoparticles were emitted from a NiO ceramic target and deposited onto the SnO_2 films. Then, the above process was repeated two times but the alumina tubes with SnO_2 were rotating around 120° each time, and then NiO/SnO_2 hollow spheres heterojunction layer was grown. Thus, the SnO_2 and NiO/SnO_2 heterojunction hollow sphere sensors were ready for further measurements. The sensor fabrication process is similar to that of SnO_2 sensor, as summarized in Fig. 1.

2.2. Characterization and gas sensing measurement

The morphology and elemental analyses of SnO_2-based hollow spheres were characterized by a field emission scanning electron microscope (FESEM, FEI QUANTA FEG250) equipped with energy dispersive X-ray spectrum (EDS, INCA Energy X-MAX-50) and transmission electron microscope (TEM JEOL-1400). The average pore size, pore volume, and specific surface area of SnO_2 hollow spheres were examined through measuring N_2 adsorption–desorption isotherm with a Micromeritics ASAP2020 apparatus. X-ray diffraction (XRD) pattern of the samples was performed on a Bruker/D8-Advance with Cu Kα radiation. The sensing properties were tested by a gas sensing measurement system (WS-30A, Weisheng Electronics, China) using ambient air as the dilute and reference gas at a relative lower humidity of 30%. The concentrations of target gases were obtained by the static gas distribution method. Test gases with calculated concentration were injected into the testing chamber by a microsyringe. Sensor response is defined as the ratio of R_a/R_g, where R_a and R_g are the resistance of the sensors in air and in target gas, respectively.

3. Results and discussion

3.1. Characterizations of SnO_2 and NiO/SnO_2 hollow spheres

The morphology of as-prepared samples was characterized via SEM and TEM microscopes. The typical morphology of SnO_2 is shown in Fig. 2(a and b). Most of samples consist of interconnected SnO_2 hollow spheres with average diameters about 300 nm. The hollow spheres show a rough and porous morphology. They are composed of numerous SnO_2 nanoparticles where can be observed

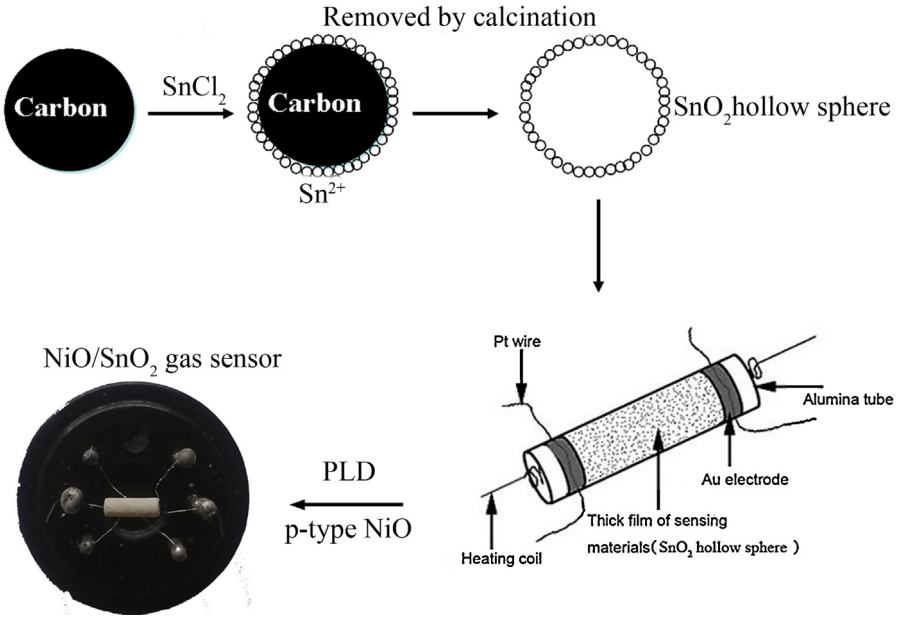

Fig. 1. Schematic for the preparation process of the gas sensors.

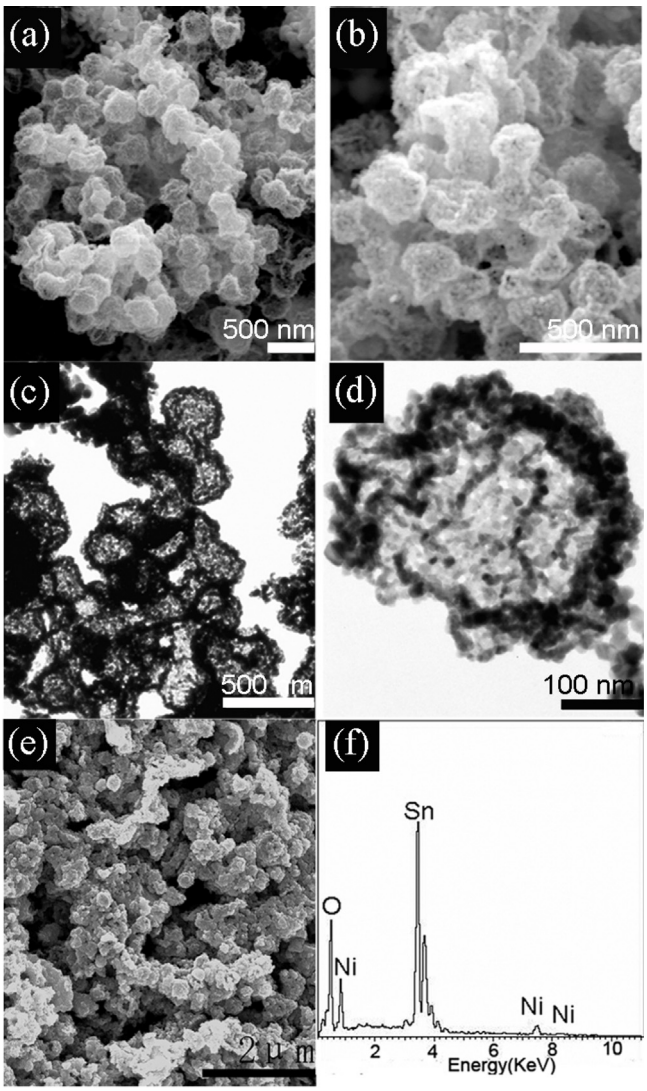

Fig. 2. (a) SEM image of SnO_2 hollow spheres, (b) TEM image of SnO_2 hollow spheres taken from (a), (c) SEM image of SnO_2 hollow spheres after a PLD growth process for NiO and (d) the corresponding EDS spectra of the sample shown in (e).

in the TEM images of Fig. 2(c and d). The rough and porous structures increase their specific surface area and may absorb more target gas molecules to improve the sensing properties. Fig. 2(e) shows the SEM images of NiO/SnO_2 hollow spheres where the SnO_2 hollow spheres have been coated on the alumina ceramic (Al_2O_3) tube and the NiO nanoparticles were implanted onto the surface of SnO_2 hollow sphere film by PLD method. The EDS spectrum shows clear peak of Ni from NiO as observed in the spectra of Fig. 2(f).

Fig. 3(a) illustrates the XRD patterns of pristine SnO_2 hollow spheres. All diffraction peaks can be well indexed to the tetragonal rutile SnO_2 structure (JCPDS card NO. 41-1445). No additional characteristic peaks are observed in the XRD pattern, proving the high purity of SnO_2 hollow spheres. When NiO nanoparticles were implanted onto SnO_2 hollow spheres by PLD process, a few additional weak peeks of NiO (JCPDS card No. 78-0643) are also observed due to its small dose, as demonstrated in Fig. 3(b).

To further investigate the inner architectures of SnO_2 hollow spheres, nitrogen adsorption–desorption analysis was used to estimate its textural properties. The nitrogen adsorption–desorption isotherm and corresponding BJH pore size distribution plots (inset) of SnO_2 hollow spheres are shown in Fig. 4. The N_2 isotherm of SnO_2

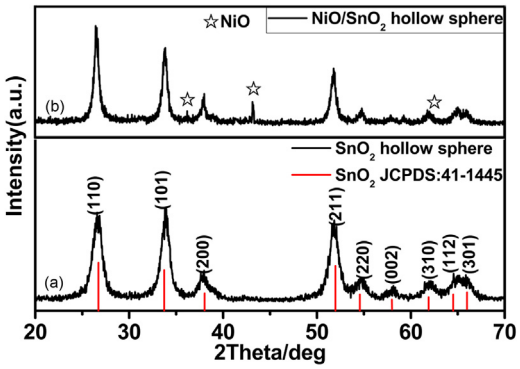

Fig. 3. XRD patterns of (a) pristine SnO_2 hollow spheres and (b) NiO/SnO_2 hollow spheres.

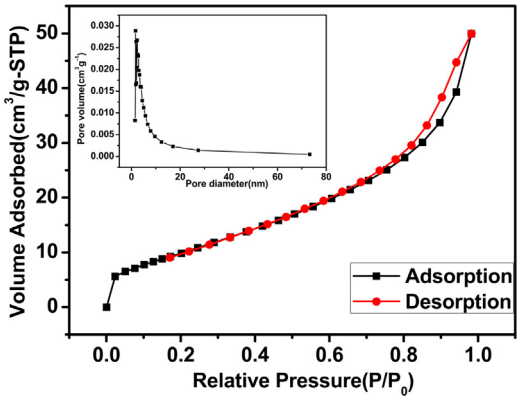

Fig. 4. Nitrogen adsorption–desorption isotherms and pore size distribution curves (inset) of the SnO_2 hollow spheres.

hollow spheres is a type-IV isotherm with a large type H3 hysteresis loop [26], and does not exhibit any limiting adsorption at high P/P_0. The products show a high BET surface area of 53.9 m^2/g. As calculated by the BJH method from the desorption branch of nitrogen isotherm, the pore size distribution (inset in Fig. 4) presents that SnO_2 hollow spheres contain an average pore size of 6.4 nm, with the small microspores in the order of 2.3 nm. The pores distributed in SnO_2 hollow spheres are also observed in TEM image (Fig. 2b) between the adjacent nanoparticles. It clearly indicates that SnO_2 hollow spheres show a high specific surface areas and a large textural porosity, which is benefit for enhancing gas sensing performance [27].

3.2. Properties comparison of SnO_2 and NiO/SnO_2 sensors

The sensing properties of prepared NiO/SnO_2 sensors toward TEA detection were initially investigated at different operating temperatures. Fig. 5 shows the response of two sensors toward 10 ppm TEA at working temperature ranging from 160 °C to 360 °C. The pristine SnO_2 sensor exhibits relatively low response of 14.5 at 220 °C and maximum response of 23.3 at 260 °C. In contrast, the response of NiO/SnO_2 sensor can reach to 30 even the working temperature as low as 160 °C. Then the response continuously increases and reaches its maximum of 48.6 at 220 °C which is about 3.4 times higher compared with SnO_2 sensor at 220 °C. Afterward, the response of NiO/SnO_2 sensor gradually decreases as the temperature further increases. This might be attributed to the competing desorption of the chemisorbed oxygen [12,28]. When the working temperature is higher than 220 °C, the rate of desorption is much higher than that of adsorption, which limits the reaction between adsorption oxygen and target gas molecules, and

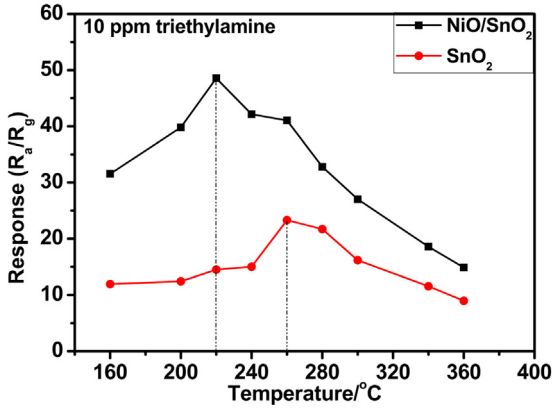

Fig. 5. Relationship between working temperature and response of pure SnO_2 sensor and NiO/SnO_2 sensor to 10 ppm TEA gas.

decreases the response of sensors. In addition, the response of pristine NiO nanoparticles toward TEA gas was also investigated, and then compared it with SnO_2 and NiO/SnO_2 sensors, as shown in the supplementary material.

Fig. 6(a) displays the response curves of sensors to different TEA concentrations from 2 ppm to 100 ppm at 220 °C. The NiO/SnO_2 sensor shows a remarkable enhancement of the sensing characteristics toward TEA. The response can reach to 270, which is much higher than that of pristine SnO_2 sensor with gas concentration of 100 ppm, as shown in Fig. 6(b). Furthermore, the high response can also be observed upon exposure to the TEA concentration as low as 2 ppm with a better response about 5.2, indicating a relatively low detection limit.

Response and recovery times are also important parameters of gas sensors and real-time detection usually needs their fast properties. The response and recovery times (T_{res} and T_{rec}) of a gas sensor are usually defined as the time takes for the resistance to reach 90% of its steady-state value after introduction or removal of the analyte gas, respectively [20]. Fig. 7(a) shows the response–recovery curve of two sensors to 10 ppm TEA at 220 °C. Both sensors can quickly respond to the TEA gas with response time of 11 s and 6 s, respectively. However, the NiO/SnO_2 sensor needs a longer time to recover than pristine SnO_2 sensor after the gas was removed. To identify the selectivity of NiO/SnO_2 sensor, we also tested its gas sensing property toward other gases including ethanol, acetone, benzene, xylene of 10 ppm at 220 °C, as shown in Fig. 7(b). The response of NiO/SnO_2 sensor is lower than 10 to other interfering gases. But, to TEA, it is as high as 48.6, indicating an excellent selectivity. A comparison of the sensing performances between our sensor and literature reports is summarized in Table 1. It is noteworthy that our sensor exhibit higher response than those reported.

Table 1
Sensing properties of NiO/SnO_2 hollow spheres and other reported gas sensors working under different operating temperatures.

Sensing material	[TEA] (ppm)	T_{sens} (°C)	Response (R_a/R_g)	Refs
SnO_2 nanorods	50	350	65	[16]
ZnO nanorods	500	150	300	[17]
NiO/ZnO nanosheets	100	320	185.1	[22]
SnO_2 flowerlike	45	350	2.97	[29]
Brick-shaped SnO_2	100	160	70	[30]
$NiFe_2O_4$ nanorods	100	175	100	[31]
NiO/SnO_2 hollow spheres	10	220	46.5	Our work
	50		163.6	
	100		267.5	

3.3. Mechanism on improved sensing properties

The generally accepted sensing mechanism for pure SnO_2 gas sensors has been well interpreted by the space-charge layer mode [4,32–34]. The basic working principle of SnO_2 gas sensors depends on the variation of resistance, caused by the chemical adsorption and desorption of gas molecules. However, the sensing mechanism will be different after the formation of P–N heterojunction at the interface of oxide semiconductors. The heterojunction interface of p–n junction should be considered to analyze the behavior of a semiconducting metal oxide composite [20]. Here, the enhancement of sensing properties to TEA could be ascribed to the formation of P–N junction between p-type NiO and n-type SnO_2. As we all know, SnO_2 mainly shows n-type conductivity by electrons and NiO displays p-type conductivity by holes. When NiO nanoparticles are implanted onto the surface of SnO_2 hollow spheres, the electrons in SnO_2 and holes in NiO diffuse in opposite direction due to the great gradient of the same carrier concentration. This further induces the formation of internal built-in electric field between their interfaces. As a result, the energy band bends in the depletion layer until the system get equalization of Fermi levels (E_F), which lead to the formation of PN junction, as shown in Fig. 8(a).

When the heterostructure sensor is exposed to air at a high temperature, the resistance of the NiO/SnO_2 in air (R_a) will be even higher than without the heterojunction (pristine SnO_2) due to the depletion region at the heterojunction interface [20]. The P–N interface contributes to the increase of the resistance, as shown in Fig. 8(b). In addition, a depletion layer will be also formed on the surface of bare SnO_2, due to the chemical adsorption of oxygen molecules which extract electrons in the bulk to become oxygen

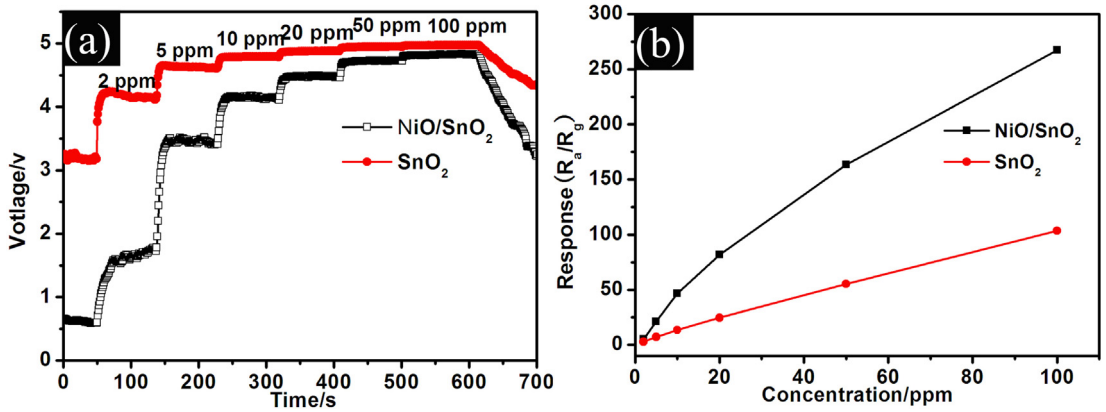

Fig. 6. (a) Responses of two sensors to TEA gas of different concentrations at 220 °C, (b) the corresponding relationship between the response and concentrations to TEA showing linear relationship over a wide concentration range.

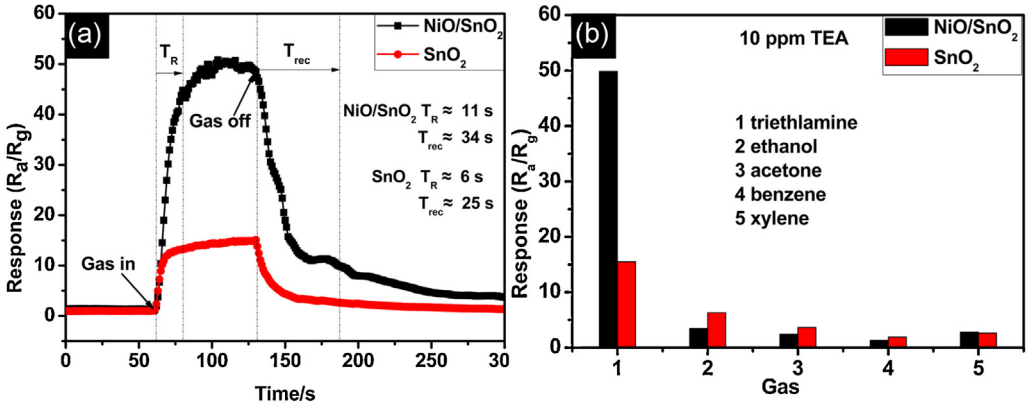

Fig. 7. (a) Response–recovery curve of the sensors to 10 ppm TEA at 220 °C and (b) the selectivity of two sensors for different target gases with same concentration at 220 °C.

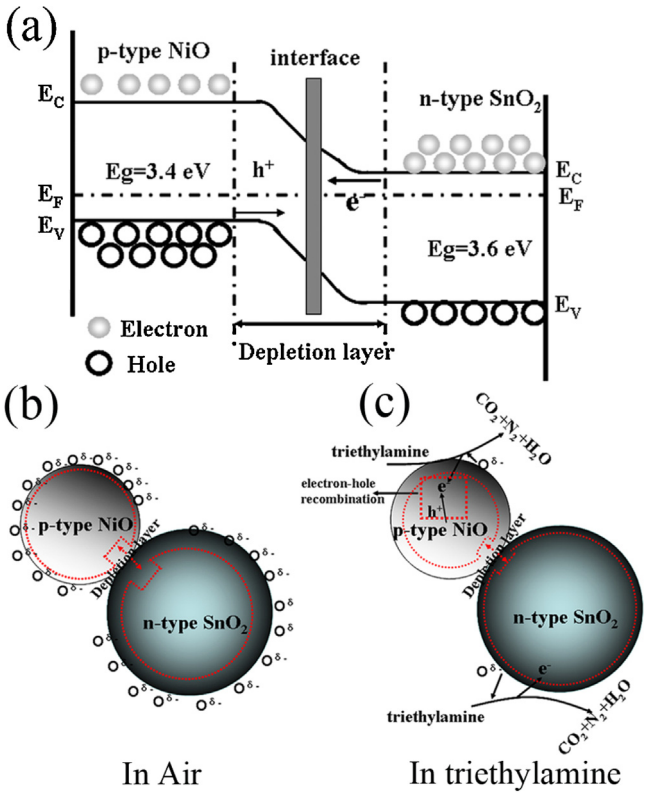

Fig. 8. (a) The energy band structure diagram of p-type NiO/n-type SnO_2 hetero-contact, (b) schematic model for the p-type NiO/n-type SnO_2 hetero-junctions based sensor when exposed to TEA gas.

ions species $O^{\delta-}$. This further increases the resistance of NiO/SnO_2. However, p-type NiO exhibits a reverse behavior in compared with n-type SnO_2. It actually forms an accumulation layer because the oxygen pulls out electrons, introducing holes, and decreases the resistance of NiO. But due to the small dose of NiO and its discontinuity of NiO film, the resistance is mainly determined by the SnO_2 and depletion regions on the heterojunction interface and the surface of SnO_2 film. However, once the NiO/SnO_2 hetero-junction sensor is exposed to TEA gas, the oxygen ions adsorbed on the sample surface react with TEA molecules and release the electrons back to SnO_2 semiconductor, causing the decrease of sensor resistance. Meanwhile, TEA release electrons to combine with holes in p-type NiO, leading to a decreased concentration of holes and an increased concentration of elections according to the Law of mass action ($n_0 \cdot p_0 = n_i^2$). Thus, the diffusion of carriers is weakened and the potential barrier height of depletion layers is also decreased, due to the reduction of concentration gradient on both sides of P–N junction. This further decreases the resistance of NiO/SnO_2 sensor. Fig. 8(c) shows a sensing mechanism model for p-type NiO/n-type SnO_2 hetero-junction based sensor when exposed to TEA gas. In short, compared with pristine SnO_2 sensor, the formation of P–N junction greatly increases the resistance of SnO_2 sensor in air and further decrease the resistance in TEA gas. Thus, based on the definition of response ($S = R_a/R_g$), the response to TEA is greatly improved due to the variation of resistance. This theoretical model can also be used to interpret other systems with their response improved by P–N junction, such as NiO–ZnO [35] and CuO–SnO_2 [36].

4. Conclusion

In conclusion, we reported a highly sensitive and selective TEA sensor by the formation of NiO/SnO_2 P–N heterostructure and the sensing mechanism was also discussed. SnO_2 hollow spheres were fabricated by a cost-effective and environment-friendly template solution method and the p-type NiO nanoparticles were successfully implanted on surface of SnO_2 hollow sphere by PLD. The as-prepared NiO/SnO_2 sensor response can get up to 48.6 when exposed to 10 ppm TEA gas. This is much higher than that of pristine SnO_2 hollow spheres and other reported TEA gas sensor. Moreover, the optimal operating temperature is down to 220 °C, and 40 °C lower than that of pristine SnO_2 hollow spheres. In comparison with pristine SnO_2 sensor, the enhanced response to TEA is mainly attributed to the variation of resistance caused by the formation of P–N junction. This work provides an effective way for design and fabrication of the gas sensors with high sensing performances.

Acknowledgments

This work is supported by NSFC (11174112, 51472110) and Shandong Provincial Natural Science Foundation (JQ201214, ZR2014JL045, BS2012CL003). The research programs from Ministry of Education of China are also acknowledged (NCET-11-1027, 213021A).

Appendix A. Supplementary data

Supplementary data associated with this article can be found, in the online version, at http://dx.doi.org/10.1016/j.snb.2015.03.015.

References

[1] L. Xu, H.J. Song, J. Hu, Y. Lv, K.L. Xu, A cataluminescence gas sensor for triethylamine based on nanosized LaF_3–CeO_2, Sens. Actuators B 169 (2012) 261–266.

[2] B. Gandu, K. Sandhya, A.G. Rao, Y.V. Swamy, Gas phase bio-filter for the removal of triethylamine (TEA) from air: microbial diversity analysis with reference to design parameters, Bioresour. Technol. 139 (2013) 155–160.
[3] T. Cai, L. Chen, Q. Ren, S. Cai, J. Zhang, The biodegradation pathway of trithylamine and its biodegradation by immobilized arthrobacter protophormiae cells, J. Hazard. Mater. 186 (2011) 59–66.
[4] E. Filippo, D. Mannob, A. Buccolieri, A. Serra, Green synthesis of sucralose-capped silver nanoparticles for fast colorimetric triethylamine detection, Sens. Actuators B 178 (2013) 1–9.
[5] H. Nohta, H. Satozono, K. Koiso, H. Yoshida, J. Ishida, M. Yamaguchi, Highly selective fluorometric determination of polyamines based on intramolecular excimer-forming derivatization with a pyrene-labeling reagent, Anal. Chem. 72 (2000) 4199–4204.
[6] B. Cheng, J.M. Russell, W.S. Shi, L. Zhang, E.T. Samulski, Large-scale, solution-phase growth of single-crystalline SnO_2 nanorods, J. Am. Chem. Soc. 126 (2004) 5972–5973.
[7] D.F. Zhang, L.D. Sun, J.L. Yin, C.H. Yan, Low-temperature fabrication of highly crystalline SnO_2 nanorods, Adv. Mater. 15 (2003) 1022–1025.
[8] G. Wang, W. Lu, J.H. Li, J. Choi, Y.S. Jeong, S.Y. Choi, J.B. Park, M.K. Ryu, K. Lee, V-shaped tin oxide nanostructures featuring a broad photocurrent signal: an effective visible-light-driven photocatalyst, Small 2 (2006) 1436–1439.
[9] W.S. Kim, Y. Hwa, J.H. Jeun, H.J. Sohn, S.H. Hong, Synthesis of SnO_2 nano hollow spheres and their size effects in lithium ion battery anode application, J. Power Sources 225 (2013) 108–112.
[10] G. Giusti, V. Consonni, E. Puyoo, D. Bellet, High performance ZnO–SnO_2:F nanocomposite transparent electrodes for energy applications, ACS Appl. Mater. Interfaces 6 (2014) 14096–14107.
[11] H.Y. Xu, X.Q. Chen, J. Zhang, J.Q. Wang, B.Q. Cao, D.L. Cui, NO_2 gas sensing with SnO_2–ZnO/PANI composite thick film fabricated from porous nanosolid, Sens. Actuators B 176 (2013) 166–173.
[12] C.H. Fang, S.Z. Wang, Q. Wang, J. Liu, B.Y. Geng, Coralloid SnO_2 with hierarchical structure and their application as recoverable gas sensors for the detection of benzaldehyde/acetone, Mater. Chem. Phys. 122 (2010) 30–34.
[13] S.L. Wang, Y. Xiao, D.Q. Shi, H.K. Liu, S.X. Dou, Fast response detection of H_2S by CuO-doped SnO_2 films prepared by electrodeposition and oxidization at low temperature, Mater. Chem. Phys. 130 (2011) 1325–1328.
[14] X.C. Ma, H.Y. Song, C.S. Guan, Interfacial oxidation–dehydration induced formation of porous SnO_2 hollow nanospheres and their gas sensing properties, Sens. Actuators B 177 (2013) 196–204.
[15] Z.P. Li, Q.Q. Zhao, W.L. Fan, J.H. Zhan, Porous SnO_2 nanospheres as sensitive gas sensors for volatile organic compounds detection, Nanoscale 3 (2011) 1646–1652.
[16] D. Wang, X.F. Chu, M.L. Gong, Gas-sensing properties of sensors based on single-crystalline SnO_2 nanorods prepared by a simple molten-salt method, Sens. Actuators B 117 (2006) 183–187.
[17] Y.Z. Lv, C.R. Li, L. Guo, F.C. Wang, Y. Xu, X.F. Chu, Triethylamine gas sensor based on ZnO nanorods prepared by a simple solution route, Sens. Actuators B 141 (2009) 85–88.
[18] F. Gyger, M. Hübner, C. Feldmann, N. Barsan, U. Weimar, Nanoscale SnO_2 hollow spheres and their application as a gas-sensing material, Chem. Mater. 22 (2010) 4821–4827.
[19] H.X. Yang, J.F. Qian, Z.X. Chen, X.P. Ai, Y.L. Cao, Multilayered nanocrystalline SnO_2 hollow microspheres synthesized by chemically induced self-assembly in the hydrothermal environment, J. Phys. Chem. C 111 (2007) 14067–14071.
[20] D.R. Miller, S.A. Akbar, P.A. Morris, Nanoscale metal oxide-based heterojunctions for gas sensing: A review, Sens. Actuators B 204 (2014) 250–272.
[21] H.-J. Kim, J.-H. Lee, Highly sensitive and selective gas sensors using p-type oxide semiconductors: Overview, Sens. Actuators B 192 (2014) 607–627.
[22] D. Ju, H. Xu, Z. Qiu, J. Guo, J. Zhang, B. Cao, Highly sensitive and selective triethylamine-sensing properties of nanosheets directly grown on ceramic tube by forming NiO/ZnO PN heterojunction, Sens. Actuators B 200 (2014) 288–296.
[23] Y.J. Hong, J.-W. Yoon, J.-H. Lee, Y.C. Kang, One-pot synthesis of Pd-loaded SnO_2 yolk–shell nanostructures for ultraselective methyl benzene sensors, Chem. Eur. J. 20 (2014) 2737–2741.
[24] H. Yang, G.H. Guai, C. Guo, Q. Song, S.P. Jiang, Y. Wang, W. Zhang, C.M. Li, NiO/graphene composite for enhanced charge separation and collection in p-type dye sensitized solar cell, J. Phys. Chem. C 115 (2011) 12209–12215.
[25] Y. Liu, G. Li, R. Mia, C. Deng, P. Gao, An environment-benign method for the synthesis of p-NiO/n-ZnO heterostructure with excellent performance for gas sensing and photocatalysis, Sens. Actuators B 191 (2014) 537–544.
[26] Z.H. Jing, J.H. Zhan, Fabrication and gas-sensing properties of porous ZnO nanoplates, Adv. Mater. 20 (2008) 4547–4551.
[27] J. Kim, W. Kim, K.J. Yong, CuO/ZnO heterostructured nanorods: photochemical synthesis and the mechanism of H_2S gas sensing, J. Phys. Chem. C 116 (2012) 15682–15691.
[28] L.J. Bie, X.N. Yan, J. Yin, Y.Q. Duan, Z.H. Yuan, Nanopillar ZnO gas sensor for hydrogen and ethanol, Sens. Actuators B 126 (2007) 604–608.
[29] B. Liu, L.H. Zhang, H. Zhao, Y. Chen, H.Q. Yang, Synthesis and sensing properties of spherical flowerlike architectures assembled with SnO_2 submicron rods, Sens. Actuators B 173 (2012) 643–651.
[30] Y.J. Xie, J.P. Du, R.H. Zhao, H.Y. Wang, H.L. Yao, Facile synthesis of hexagonal brick-shaped SnO_2 and its gas sensing toward triethylamine, J. Environ. Chem. Eng. 1 (2013) 1380–1384.
[31] X.F. Chu, D.L. Jiang, C.M. Zheng, The preparation and gas-sensing properties of $NiFe_2O_4$ nanocubes and nanorods, Sens. Actuators B 123 (2007) 793–797.
[32] H.C. Chiu, C.S. Yeh, Hydrothermal synthesis of SnO_2 nanoparticles and their gas-sensing of alcohol, J. Phys. Chem. C 111 (2007) 7256–7259.
[33] Z.J. Wang, Z.Y. Li, J.H. Sun, H.N. Zhang, W. Wang, W. Zheng, C. Wang, Improved hydrogen monitoring properties based on p-NiO/n-SnO_2 heterojunction composite nanofibers, J. Phys. Chem. C 114 (2010) 6100–6105.
[34] Y.J. Chen, L. Yu, D.D. Feng, M. Zhuo, M. Zhang, E.D. Zhang, Z. Xu, Q.H. Li, T.H. Wang, Superior ethanol-sensing properties based on Ni-doped SnO_2 p–n heterojunction hollow spheres, Sens. Actuators B 166–167 (2012) 61–67.
[35] L. Xu, R.F. Zheng, S.H. Liu, J. Song, J.S. Chen, B. Dong, H.W. Song, NiO@ZnO heterostructured nanotubes: coelectrospinning fabrication, characterization, and highly enhanced gas sensing properties, Inorg. Chem. 51 (2012) 7733–7740.
[36] Y. Zhao, X.L. He, J.P. Li, X.G. Gao, J. Jia, Porous CuO/SnO_2 composite nanofibers fabricated by electrospinning and their H_2S sensing properties, Sens. Actuators B 165 (2012) 82–87.

Biographies

Dianxing Ju is a graduate student focusing on ZnO semiconductor gas sensor for master degree at University of Jinan. He was awarded a B.Sc. degree in materials science and engineering from the same university in 2012.

Hongyan Xu is an Associate Professor at School of Materials Science and Engineering, University of Jinan. Her main research interests are the synthesis and fabrication of semiconductor nanomaterials and conductive polymer composite chemical gas sensors.

Qi Xu is a graduate student focusing on ZnO and SnO_2 semiconductor gas sensor for master degree at University of Jinan. She was awarded a B.Sc. degree in materials science and engineering from the same university in 2014.

Haibo Gong is a lecture at School of Materials Science and Engineering, University of Jinan. His main research interests include the fabrication of semiconducting oxide thin films and their applications in light-emitting diodes and the third generation solar cells.

Zhiwen Qiu is a Ph.D. student focusing on PLD growth oxide film at University of Jinan. She was awarded a bachelor and Master degree in materials science and engineering from the same university in 2011 and 2014.

Jing Guo is a graduate student focusing on SnO_2 gas sensor and lithium battery for master degree at University of Jinan. She was awarded a B.Sc. degree in materials science and engineering from the same university in 2012.

Jun Zhang obtained his Ph.D. of Chemistry from Nankai University in 2011 and now is a lecture with University of Jinan. His research is focused on nanomaterials and advanced applications in gas sensing and energy conversion devices.

Bingqiang Cao is a Taishan Scholar Professor for material physics with University of Jinan. He leads the group focusing on semiconducting oxide thin films, heterostructures, nanostructures, and related devices.